

AD-A179 152

Fourier Transform Infrared Spectroscopic Study of Thermal and Electrical Aging in Polyurethane

R. S. BRETZLAFF and S. L. SANDLIN
Materials Sciences Laboratory
Laboratory Operations
The Aerospace Corporation
El Segundo, CA 90245

20 March 1987

APPROVED FOR PUBLIC RELEASE;
DISTRIBUTION UNLIMITED

DTIC
SELECTED
APR 16 1987
S E D
E

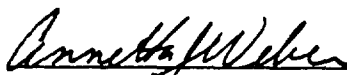
Prepared for
SPACE DIVISION
AIR FORCE SYSTEMS COMMAND
Los Angeles Air Force Station
P.O. Box 92960, Worldway Postal Center
Los Angeles, CA 90009-2960

This report was submitted by The Aerospace Corporation, El Segundo, CA 90245, under Contract No. F04701-85-C-0086 with the Space Division, P.O. Box 92960, Worldway Postal Center, Los Angeles, CA 90009. It was reviewed and approved for The Aerospace Corporation by R.W. Fillers, Director, Materials Sciences Laboratory.

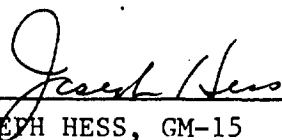
Capt Annetta Weber/YNSA was the project officer for the Mission-Oriented Investigation and Experimentation (MOIE) Program.

This report has been reviewed by the Public Affairs Office (PAS) and is releasable to the National Technical Information Service (NTIS). At NTIS, it will be available to the general public, including foreign nationals.

This technical report has been reviewed and is approved for publication. Publication of this report does not constitute Air Force approval of the report's findings or conclusions. It is published only for the exchange and stimulation of ideas.



ANNETTA WEBER, Capt, USAF
MOIE Project Officer
SD/YNSA



JOSEPH HESS, GM-15
Director, AFSTC West Coast Office
AFSTC/WCO OL-AB

UNCLASSIFIED

SECURITY CLASSIFICATION OF THIS PAGE (When Data Entered)

REPORT DOCUMENTATION PAGE		READ INSTRUCTIONS BEFORE COMPLETING FORM
1. REPORT NUMBER SD-TR-87-04	2. GOVT ACCESSION NO. ADAM9152	3. RECIPIENT'S CATALOG NUMBER
4. TITLE (and Subtitle) Fourier Transform Infrared Spectroscopic Study of Thermal and Electrical Aging in Polyurethane		5. TYPE OF REPORT & PERIOD COVERED
		6. PERFORMING ORG. REPORT NUMBER TR-0086 (6925-08)-4
7. AUTHOR(s) Robert S. Brétzlaff and S. L. Sandlin		8. CONTRACT OR GRANT NUMBER(s) F04701-85-C-0086-P00016
9. PERFORMING ORGANIZATION NAME AND ADDRESS The Aerospace Corporation El Segundo, CA 90245		10. PROGRAM ELEMENT, PROJECT, TASK AREA & WORK UNIT NUMBERS
11. CONTROLLING OFFICE NAME AND ADDRESS Space Division Los Angeles Air Force Station Los Angeles, CA 90009		12. REPORT DATE 20 March 1987
		13. NUMBER OF PAGES 41
14. MONITORING AGENCY NAME & ADDRESS (if different from Controlling Office)		15. SECURITY CLASS. (of this report) Unclassified
		15a. DECLASSIFICATION/DOWNGRADING SCHEDULE
16. DISTRIBUTION STATEMENT (of this Report) Approved for public release; distribution unlimited.		
17. DISTRIBUTION STATEMENT (of the abstract entered in Block 20, if different from Report)		
18. SUPPLEMENTARY NOTES		
19. KEY WORDS (Continue on reverse side if necessary and identify by block number) aging, molecular environment, electrical insulation, polymer dielectric, encapsulation, polyurethane, FTIR,		
20. ABSTRACT (Continue on reverse side if necessary and identify by block number) Many different polymeric insulations, such as silicones, epoxies, polyethylenes, etc., are in use. Unfortunately, these materials exhibit decreasing resistance to electrical stress with time. In order to characterize these degradation processes and to suggest materials changes that will ameliorate them, we are developing Fourier transform infrared spectroscopy (FTIR) techniques to look for molecular changes that occur before breakdown and which may therefore be used as a "distant early-warning line" for impending breakdown. (Key...)		

UNCLASSIFIED

SECURITY CLASSIFICATION OF THIS PAGE(When Data Entered)

19. KEY WORDS (Continued)

20. ABSTRACT (Continued)

Polyurethane was studied initially because of its widespread application in space.

It was observed that FTIR absorbance changes occur during the so-called "formative stage" before catastrophic breakdown. Our tests on the commercial polyurethane Uralane 5753 included physical, or shelf-life, aging for 4 months at room temperature, thermal aging at 100°C for 1 hr in air, and electrical aging of a 0.125-in.-thick slab at 24 kV dc for 3 months. Particularly strong absorbance decreases were noted in the urethane N-H bending and C-N stretching modes (1220 and 1522 cm^{-1}), and in the C=O stretching modes (1712 and 1735 cm^{-1}). N-H stretching modes at 3423 , 3370 , and 3327 cm^{-1} were unaffected. Furthermore, CH_2 symmetric and antisymmetric stretching frequencies at 2921 and 2845 cm^{-1} showed strong decreases, as did the 966 cm^{-1} trans 1,4-polybutadiene band. These changes are consistent with a time-dependent chain conformation or environment. Some differences in detail between the results of the three aging procedures were noted.

It is well known that electrical aging causes reduced material resistance to electric stress. It is concluded here that physical, thermal, and electrical aging cause characteristic infrared peak absorbance changes and that a significant correlation exists between these spectral changes, and the reduced resistance to electrical stress.

UNCLASSIFIED

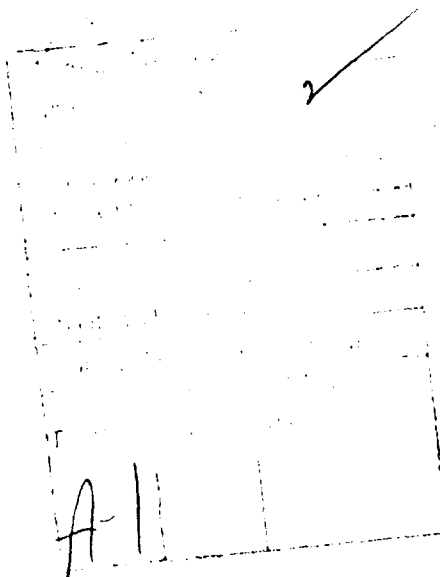
SECURITY CLASSIFICATION OF THIS PAGE(When Data Entered)

PREFACE

The authors wish to thank Gloria To for the operation of the FTIR and Bob Shenk for the DSC work.

CONTENTS

PREFACE.....	1
I. INTRODUCTION.....	9
II. EXPERIMENTAL PROCEDURE.....	11
A. Material.....	11
B. Measurement Technique.....	12
III. EXPERIMENTAL RESULTS.....	15
A. DSC Results.....	15
B. Infrared Results.....	15
IV. DISCUSSION.....	35
A. Chain Motion, Chain Conformation, and Reduction in IR Activity.....	35
B. Molecular-Environmental Explanation for Charging Infrared Activity.....	37
C. Impact of Molecular Motion Upon Electronic Properties and Electrical Tree Nucleation.....	38
V. SUMMARY AND CONCLUSIONS.....	41
REFERENCES.....	45



FIGURES

1a.	DSC Trace for Uralane 5753, Showing Two Transitions.....	16
1b.	High-Temperature DSC Trace for Uralane, Showing a Broad Exotherm between 160 and 220°C.....	17
2a.	Uralane 5753 Survey Infrared Absorption Spectrum (Lower Frequencies).....	18
2b.	Uralane 5753 Survey Infrared Absorption Spectrum (Higher Frequencies).....	19
3a.	Uralane 5753 Physical-Aging Infrared Difference Spectrum (Lower Frequencies).....	24
3b.	Uralane 5753 Physical-Aging Infrared Difference Spectrum (Higher Frequencies).....	25
3c.	Uralane 5753 Physical-Aging Infrared Difference Spectrum in the Isocyanite Region.....	26
4a.	Uralane 5753 Thermal-Aging Infrared Difference Spectrum (Lower Frequencies).....	28
4b.	Uralane 5753 Thermal-Aging Infrared Difference Spectrum (Higher Frequencies).....	29
4c.	Uralane 5753 Thermal-Aging Infrared Difference Spectrum in the Isocyanate Region.....	30
5a.	Uralane 5753 Electrical-Aging Infrared Difference Spectrum (Lower Frequencies).....	31
5b.	Uralane 5753 Electrical-Aging Infrared Difference Spectrum (Higher Frequencies).....	32
5c.	Uralane 5753 Electrical-Aging Infrared Difference Spectrum in the Isocyanate Region.....	33

TABLES

1.	Uralane 5753 Survey Spectrum and Aging Results.....	20
2.	Survey Spectrum and Aging Results, Grouped According to Phase.....	22

I. INTRODUCTION

Partial discharge testing¹ of polyurethane insulation having intentionally introduced macroscopic defects reveals signatures related to the type of defect. However, although careful fabrication can result in defect-free insulation, a perfectly fabricated satellite electronic power conditioner (EPC) or traveling wave tube amplifier (TWTA) may function for years before failing because of a shorted-out component. By extension, it may be expected that the dielectrics in high-voltage transmission lines used in future space missions may be even more susceptible to these problems. If the insulation is thought of as an inert material, i.e., one with time-independent properties, then such failures are not explainable by means of a causal series of events in the material. Some hypothetical external failure mechanism such as outgassing contamination might be investigated in order to explain a shorted-out device.

However, it has been noted in many journal articles²⁻²¹ that many physical and chemical changes may occur before breakdown. It is not only possible, but also highly likely, that events intrinsic to the insulating material result in electrical breakdown after an indefinite lifetime. A polymeric dielectric is more accurately thought of as a seething molecular and electronic cauldron, one that gradually drifts in the direction of lesser resistance to normal electrical stress. After a time, which appears indefinite only as long as the system has not been adequately characterized, the constant electrical stress shorts out the degraded insulation. The conduction path through the insulation is often referred to as an "electrical tree" because of its branched appearance.

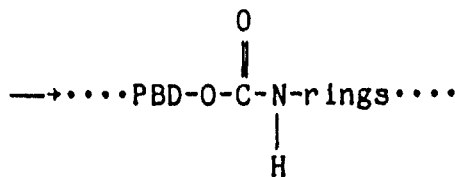
It is generally agreed now that field emission of electrons from field concentration sites (on the electrodes) into the polymer plays a central role in electrical breakdown. Hot electrons in the (Frohlich) low-temperature regime or slightly-above-thermal electrons in the high-temperature regime mediate an energy transfer from field to lattice.⁵ The details are complicated because of the wide range of possibilities for the following interactions:

- (a) electric field-electron
- (b) electron-phonon
- (c) electron-electron
- (d) electron scattering from trap sites
- (e) injected electron-space charge

In addition, polymer mobility, free volume, and microstructure play a role in complicating the situation.

Whatever the mechanism, it does seem that polymer molecules are eventually ionized and free radicals are formed. Such radicals are known to be capable of diffusing for a time, ultimately causing chain scission and the release of gaseous by-products. The formation of a certain critical mass of gas would correspond to the tree nucleation phase, followed by the relatively rapid (because aided by high gas pressures) tree-growth and shorting-out stages. It is the widely variable duration of the competing physical processes before the critical mass of gas is formed (Budenstein's "formative stage")²¹ which is critical for our investigation of indefinite lifetime effects.

The Mitsui et al. paper¹⁵ suggested our experimental approach. FTIR analysis of the stressed dielectric during the formative stage will be interpreted in terms of hypothesized chemical pathways for degradation. In this report we wish to demonstrate that measurable FTIR effects exist in one commercial polyurethane, and to discuss some qualitative features of physical thermal, and electrical aging.



Only urethane groups (no urea groups) are present in this material. The trans-1,4-PBD configuration is drawn because it appears most prominently in the infrared evidence discussed below. Some cis-1,4-PBD and 1,2-PBD bands will also be seen.

B. MEASUREMENT TECHNIQUE

Sample thermal characterization was obtained with a Mettler TA 3000 differential scanning calorimeter (DSC) on 20-mg samples of Uralane at 10°C/min. from -100°C to 200°C under nitrogen.

Uralane 5753 specimens (1.5 mil nominal thickness) for transmission infrared analysis were microtomed from 0.125-in. slabs. The Uralane slab was freshly prepared for a series of physical-, thermal-, and electrical-aging experiments. It is well known²⁵ that microtoming causes chain scission and reduction of molecular weight in uncrosslinked systems, and we do not doubt that some such changes occur here. However, difference spectra, described below, of similar samples prepared at different times were always observed to give null results (i.e., zero absorbance for all frequencies, to within experimental error). Therefore we believe that no significant sample-preparation artifacts appear in our difference spectra, although other measurement techniques may reveal a difference in molecular weight.

A Nicolet MX-1 Fourier transform infrared spectrometer (FTIR) with a Harrick 4× beam condenser were used for unpolarized transmission measurements. Measurement times between 1 and 4 min (between 32 and 128 scans) were used to obtain suitable spectra at 2 cm⁻¹ resolution with Happ Genzel apodization.

Infrared spectra were obtained before and after three aging experiments. Physical, or shelf-life, aging was conducted on freshly prepared Uralane 5753 for 4 months at room temperature. Thermal aging of the fresh Uralane 5753 at 100°C for 1 hr was performed. Finally, a fresh Uralane 5753

slab was aged between parallel electrodes at 24 kVdc for 3 months. This slab was 0.125-in. thick and extended well beyond the electrode area, i.e., some of the material saw no electric field. This experiment was conducted while the electrodes and the sample were immersed in Fluorinert to prevent breakdown from the electrode leads.

Difference spectra of the final less the initial spectra were obtained. The validity of the subtraction technique has been established in previous reports.^{26,27}

III. EXPERIMENTAL RESULTS

A. DSC RESULTS

Low-temperature Uralane 5753 results are shown in Fig. 1a. Two thermal events are seen at -72 and -17°C. High-temperature Uralane 5753 results (Fig. 1b) show a broad exotherm in the 160 to 220°C range. The final decomposition of Uralane (endothermic event) evidently does not occur until above 250°C at 10°C/min. The -72°C transition is the T_g of the PBD soft phase, in agreement with the assignment of Hsu et al. in a related system.²⁸ The -17°C transition is a hard-segment glass transition. The broad 160 to 220°C exotherm possibly corresponds to a paracrystallization (formation or reordering of small, imperfect crystals in the hard domains) upon heating.

B. INFRARED RESULTS

1. SURVEY SPECTRUM

The Uralane 5753 survey spectrum is shown in Fig. 2a and b. The bands are listed and identified in Tables 1 and 2 according to the references cited. This file was also used as the reference file for the physical- and thermal-aging experiments described below.

2. PHYSICAL AGING

The FTIR difference spectrum of the 4-month-aged Uralane 5753 ("sample file") less the as-cast material ("reference file") is shown in Fig. 3a, b, and c. (The "sample file" and "reference file" are the Nicolet designations for storage areas in the FTIR data system.) The "FCR number," or multiplier for the reference file before it is subtracted from the sample file (to account for sample thickness variations), was selected as follows: The raster screen was set for -0.2 to 0.2 absorbance units, and the FCR number was varied interactively while the raster display of the difference spectrum was observed. The criteria of success for the subtraction were (1) the elimination or minimization of as many peaks in the difference spectrum as possible, and (2) the attainment of a flat and smooth baseline close to zero absorbance. Although these criteria are not required to be self-consistent as a

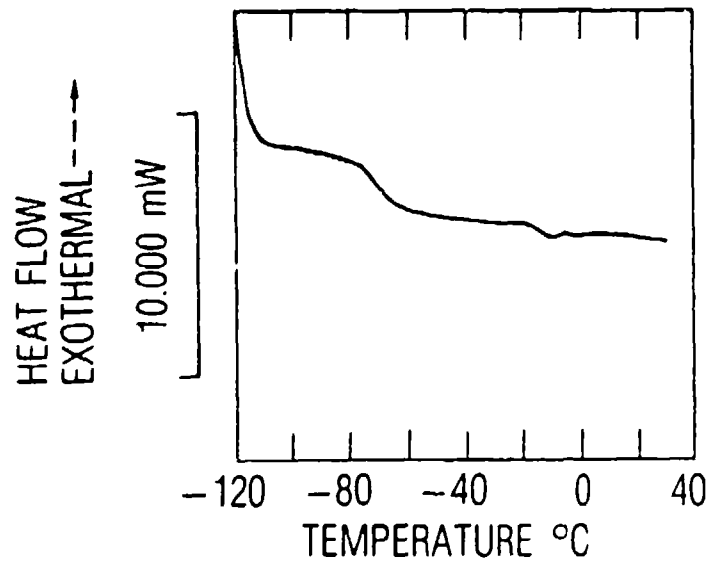


Fig. 1a. DSC Trace for Uralane 5753, Showing Two Transitions

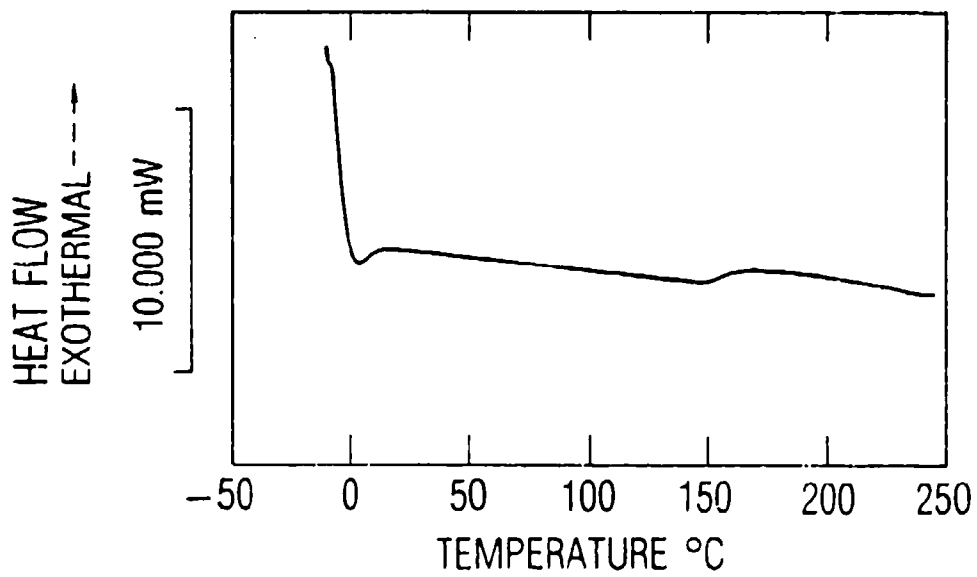


Fig. 1b. High-Temperature DSC Trace for Uralane, Showing a Broad Exotherm between 160 and 220°C

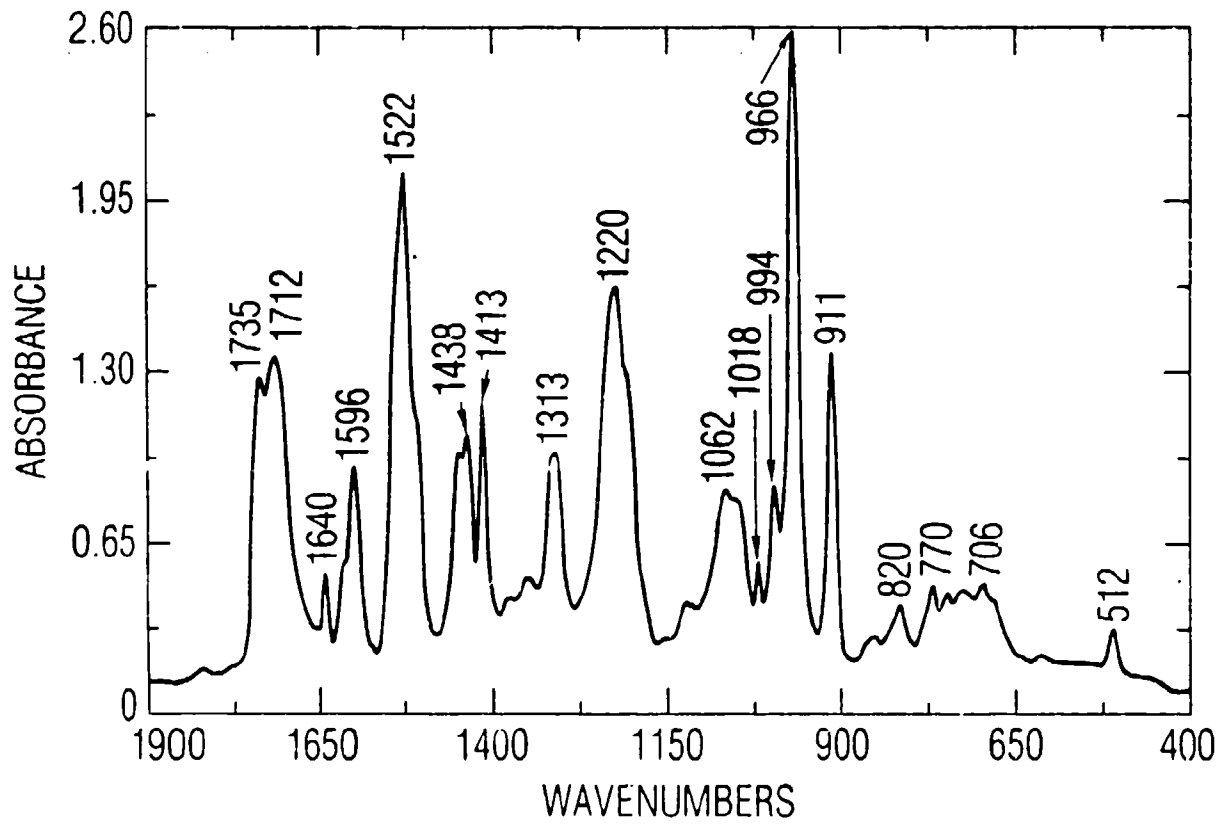


Fig. 2a. Uralane 5753 Survey Infrared Absorption Spectrum (Lower Frequencies)

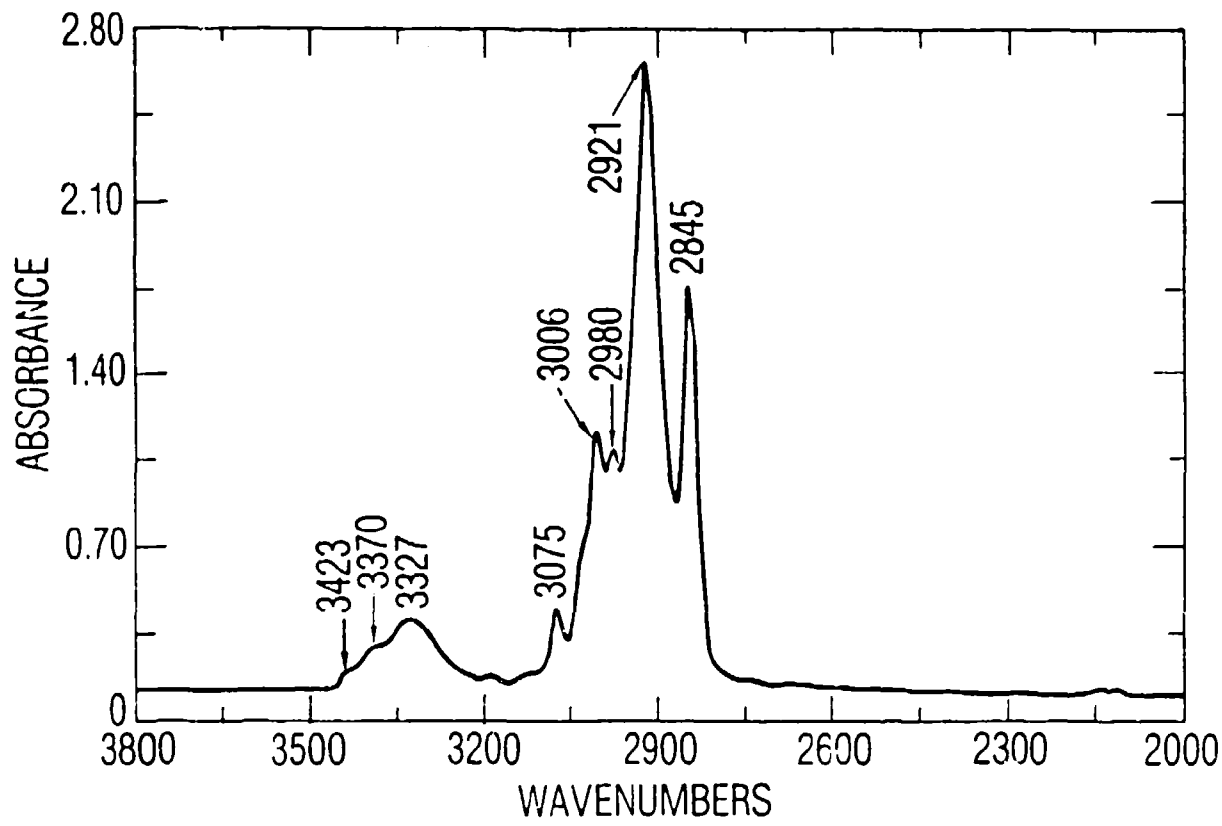


Fig. 2b. Uralane 5753 Survey Infrared Absorption Spectrum (Higher Frequencies)

Table 1. Uralane 5753 Survey Spectrum and Aging Results

Band Peak, a cm ⁻¹	Band Strength ^b	Ref ^c	Phase ^d	Assignment ^e	Physical Aging ^f	Thermal Aging ^g	Electrical Aging ^h
3423	SH	1	UR	v(N-H) free, 1	nc	nc	nc
3370	SH	-	UR	v(N-H) free, 2	nc	nc	nc
3327	S	1	UR	v((N-H) bonded	nc	nc	nc
3075	W	2	1,2,-PBD	v(=CH ₂) (vinyl)	nc	nc	nc
3006	W	2	cis-1,4-PBD	v(CH=CH)	-m	-m	-m
2980	W	2	1,2-PBD	v(CH=CH) (vinyl)	-m	-m	-m
2921	VS	1,2,3	any PBD	v _a (CH ₂)	-vs(-0.8)	vs(-2.4)	-vs _i
2845	VS	1,2,3	any PBD	v _S (CH ₂)	-s	-s	-m
2295	VW	3	ISO	v(-N=C=O) aged	+VW	-VW	-VW
2137	VW	3	ISO	v(-N=C=O) fresh	-W	-VW	+W
2012	VW	3	ISO	v(-N=C=O) fresh	-W	-VW	+W
1735	S	1	UR	v(C-O) free	-m	-m	-m
1712	VS	1	UP	v(C=O) bonded	-m	-m	-m
1540	W	2	1,2-PBD	v(C=C) (vinyl)	-W	nc	nc
1526	m	1	UR	v(C=C) (phenyl)	-W	-W	-W
1522	VS	1	UR	γ _b (N-H)+γ(C-N)	-S	-S	-S
1448	m	1,2	(?)-PBD	δ(CH ₂)	-m	-m	-W
1438	m	1,2	(?)-PBD	δ(CH ₂)	-m	-m	-m
1413	m	2	1,2-PBD	δ(=CH) _i p	-m	-W	-W
1313	m	2	trans-1,4-PBD	γ _b (HCC) _i p	-m	-W	-W
1220	VS	1	UR	γ _b (N-H)+v(C-N)	-S	-S	-m
1092	m	1,2	trans-1,4-PBD	v _b (C-C)	-W	-W	-VW
1018	W	2	trans-1,4-PBD	γ _b ^S (CCC)	nc	-W	-VW

Table 1. Uralane 5753 Survey Spectrum and Aging Results (Continued)

Band Peak, ^a cm ⁻¹	Band Strength ^b	Ref ^c	Phased ^d	Assignment ^e	Physical Aging ^f	Thermal Aging ^g	Electrical Aging ^h
994	w	1,2,3	(?)-PBD	no agreement	-vw	-w	-vw
956	vs	1,2	trans-1,4-PBD	$\gamma_w (=CH)$ op	-vs(-0.78)	-vs(-2.3)	-vs(-0.64)
911	s	1,3	1,2-PBD	$\gamma_w (=CH_2)$ op	-m	-m	-m
820	w	1,2	(?)-PBD	no agreement	nc	nc	nc
770	w	1	UR	$\gamma_b (COO)$ op	nc	nc	nc
735	w	3	cis-1,4-PBD	$\delta (=CH)$ op	nc	nc	nc
721	w	1	any PSD	$\gamma'_p (CH_2)$ op	nc	nc	nc

^afrom Fig. 2a, b.

^bvs, s, m, w, vw, sh = very strong, strong, medium, weak, very weak, and shoulder, respectively.

^cref = C. M. Brunette et al. (Ref. 28).

^d"2" = S. W. Cornell and J. L. Koenig (Ref. 29).

^e"3" = Sadtler, Ref. (30), p. 63.

^fUR, ISO, 1,2-PBD, trans-1,4-PBD, cis-1,3-PBD = urethane, isocyanate, and the three isomers of polybutadiene: 1,2; trans-1,4 and cis-1,4.

^gv, a, s, γ_b , δ , ip, op, γ_w , γ_c = stretch, antisymmetric, symmetric, bend, deformation, in-plane, out-of-plane, wag, and rock, respectively.

^hfrom Fig. 3a, b, c.

ⁱfrom Fig. 4a, b, c.

^jfrom Fig. 5a, b, c.

^kSubtraction artifacts due to sample thickness.

Table 2. Survey Spectrum and Aging Results,
Grouped According to Phase

Band Peak, cm^{-1}	Band Strength ^a	Ref.	Assignment	Physical Aging	Thermal Aging	Electrical Aging
GENERIC PBD						
2921	vs	1,2,3	$\nu_a(\text{CH}_2)$	-vs(-0.8)	-vs(-2.4)	-vs
2845	vs	1,2,3	$\nu_s(\text{CH}_2)$	-s	-s	-m
1448/1438	m	1,2	$\delta(\text{CH}_2)$	-m	-m	-w
994	w	1,2,3	no agreement	-vw	-vw	-vw
820	w	1,2	no agreement	nc	nc	nc
721	w	1	$\gamma_r(\text{CH}_2)$	nc	nc	nc
TRANS-1,4-PBD						
1313	M	2	$\gamma_b(\text{HCC})$	-m	-w	-w
1062	m	1,2	$\nu_s(\text{CCC})$	-w	-w	-vw
1018	w	2	$\gamma_s(\text{CCC})$	nc	-vw	-vw
966	vs	1,2	$\gamma_w(\text{=CH})_{op}$	-vs(-0.78)	-vs(-2.3)	-vs(-0.64)
CIS-1,4-PBD						
3006	w	2	$\nu(\text{CH=CH})$	-m	-m	-m
735	w	3	$\delta(\text{=CH})_{op}$	nc	nc	nc
1,2-PBD						
3075	w	2	$\nu(\text{=CH}_2)$	nc	nc	nc
2980	w	2	$\nu(\text{CII=CH})$	-m	-m	-m
1640	w	2	$\nu(\text{C=C})$	-w	nc	nc
1413	m	2	$\delta(\text{=CH})$	-m	-w	-w
911	s	1,3	$\gamma_w(\text{=CH}_2)_{op}$	-m	-m	-m
URETHANE						
3423	sh	1	$\nu(\text{N-H})$ free,1	nc	nc	nc
3370	sh	-	$\nu(\text{N-H})$ free,2	nc	nc	nc
3327	sh	1	$\nu(\text{N-H})$ bonded	nc	nc	nc
1735	s	1	$\nu(\text{C=O})$ free	-m	-m	-m
1712	vs	1	$\nu(\text{C=O})$ bonded	-m	-m	-m
1596	m	1	$\nu(\text{C=C})$ phenyl	-w	-w	-w
1522	vs	1	$\gamma_b(\text{N-H})+\nu(\text{C-N})$	-s	-s	-s
1220	vs	1	$\gamma_b(\text{N-H})+\nu(\text{C-N})$	-s	-s	-m
770	w	1	$\gamma_b(\text{COO})_{op}$	nc	nc	nc

^aSee notes from Table 1.

matter of logic, in fact they never conflicted in this or any other aging study. In this case, FCR = 1.14.

Whereas we had expected some positive-going and some negative-going changes, corresponding to our a priori expectation of continuing chemical curing reactions and/or time-dependent chain rearrangements, the observations in Fig. 3a, b, and c are remarkable indeed. With the single exception of some weak bands near 1375 cm^{-1} , all of the bands that change go negative. Even the 2921 and 2845 cm^{-1} bands, which are often used as internal thickness standards because of the customarily assumed environmental independence of the CH_2 ν_s and ν_a modes, show strong decreases. Nevertheless, we believe that the FCR number selection algorithm stated above adequately removes the effects of difference in thickness between the microtomed specimens of original and aged materials for the following reasons:

1. A flat and smooth baseline close to the zero-absorbance level was achieved.
2. Some bands do subtract out to zero absorbance. For example, all the bands below 900 cm^{-1} subtract out, as well as the 3423 , 3370 , 3327 , and 3075 cm^{-1} bands. These bands are immediately adjacent to the 966 , 2921 , and 2845 cm^{-1} bands, which do decrease strongly.
3. The ratio of the absolute values of the strongest peaks (911 , 966 , 1220 , 1522 , and 1712 cm^{-1}) is different in the case of the survey spectrum (Fig. 2a) and of the difference spectrum (Fig. 3a). This ratio is $0.51:1.0:0.60:0.77:0.50$ for the survey spectrum and $0.15:1.0:0.31:0.61:0.11$ for the difference spectrum. Thus, the difference spectrum does not arise merely as the result of "oversubtraction," i.e., selection of a too-large FCR number.
4. In experiments described elsewhere³¹, aging was carried out on a microtomed slice held in an infrared holder. Thus the same area was probed by infrared radiation after many different aging times. Initially, the entire difference spectrum was extremely close to the zero baseline, to within experimental error. Only as time passed did some difference peaks grow into the spectrum. In oxidative experiments some positive-going changes were noted, as expected. Thus, this technique is capable of detecting null results, when in fact they occur.

In summary, we do accept the difference spectra changes in Fig. 3a, b, and c as legitimate. The results are listed in Table 1, column 6, and

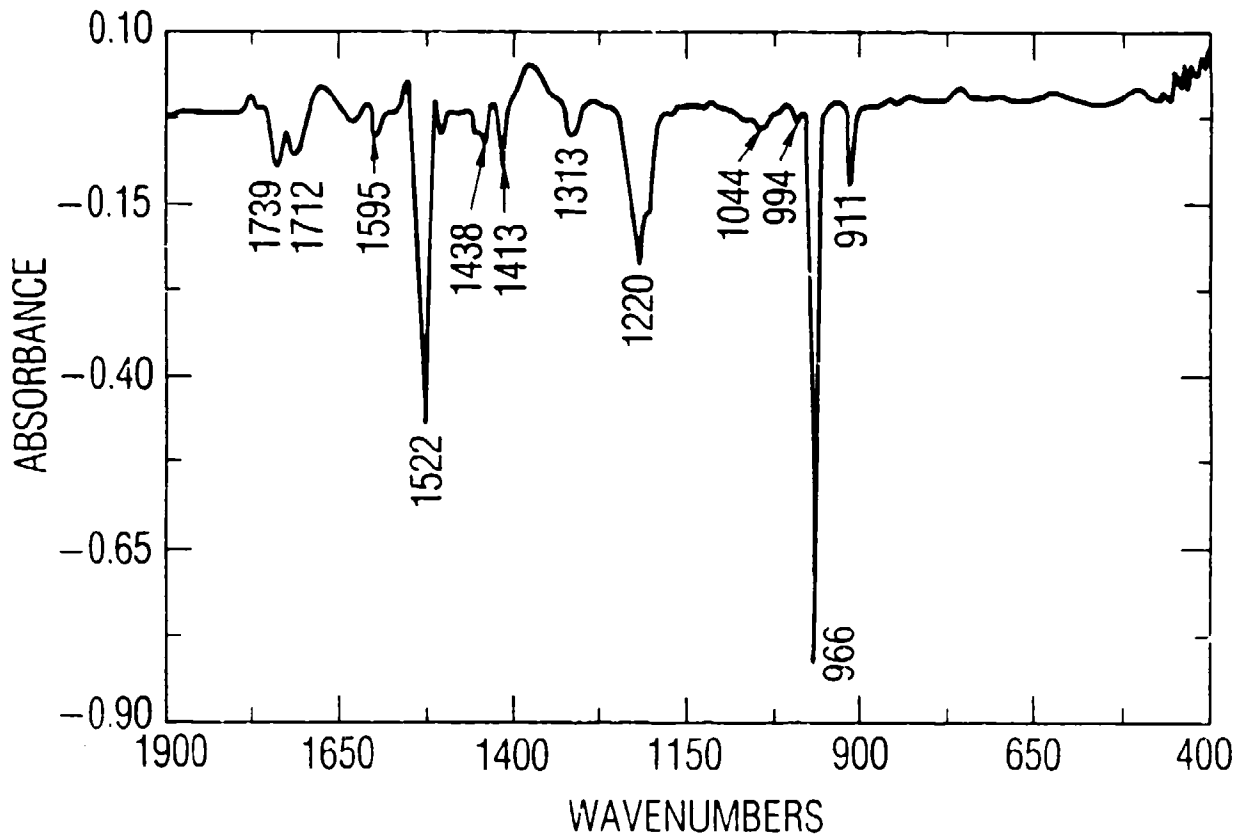


Fig. 3a. Uralane 5753 Physical-Aging Infrared Difference Spectrum (Lower Frequencies)

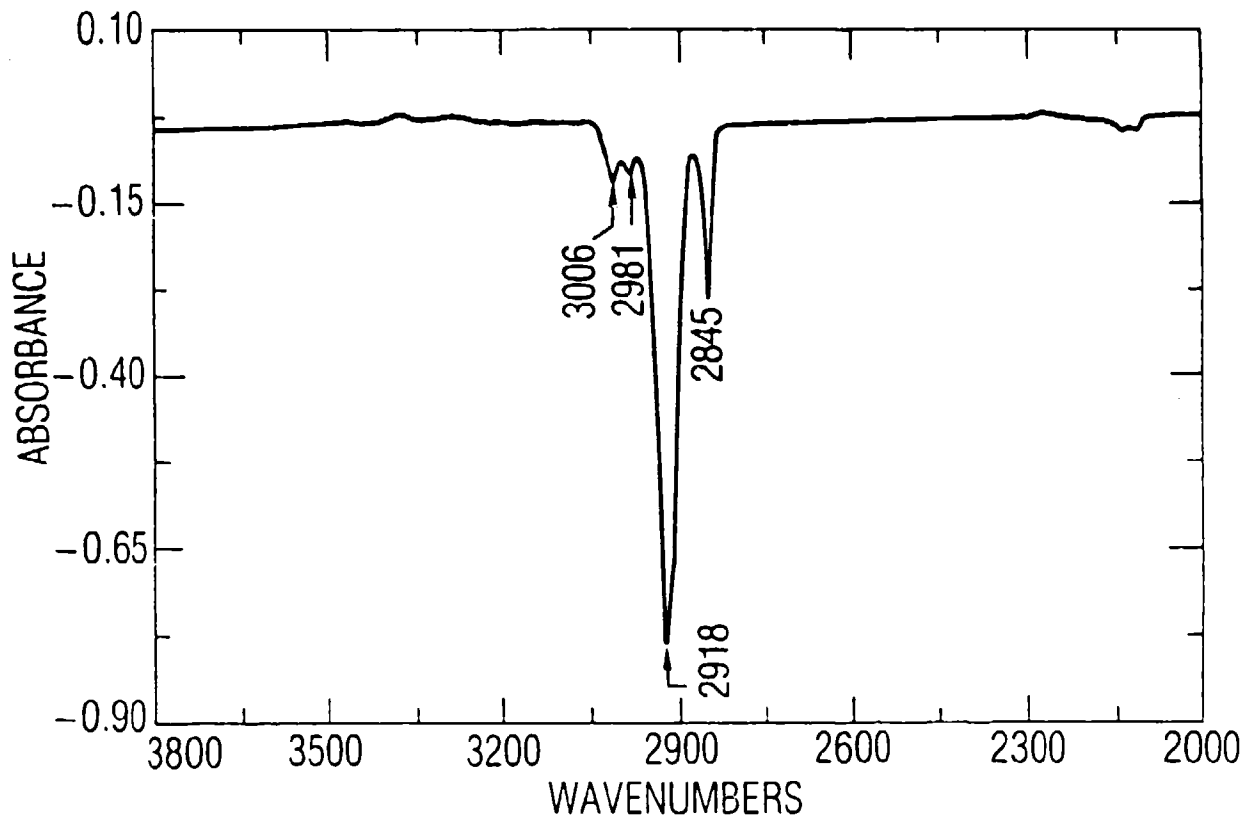


Fig. 3b. Uralane 5753 Physical-Aging Infrared Difference Spectrum (Higher Frequencies)

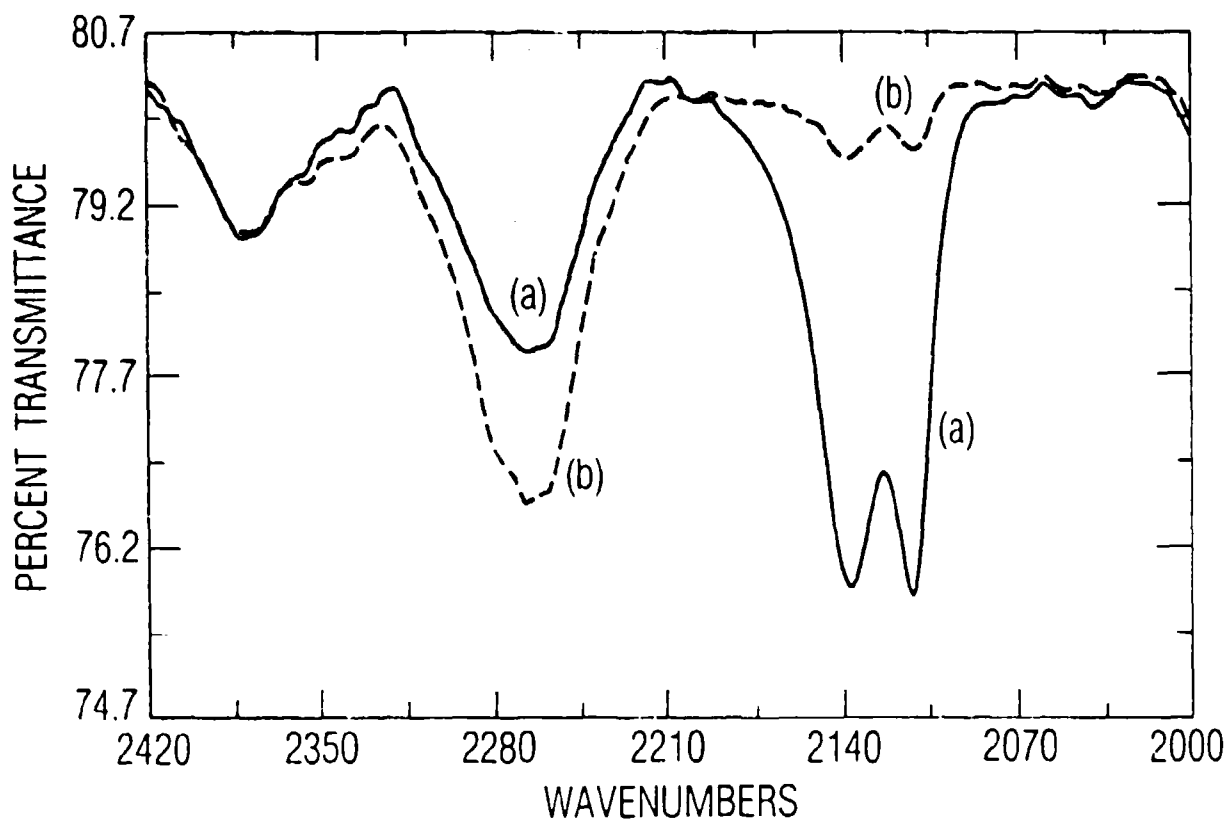


Fig. 3c. Uralane 5753 Physical-Aging Infrared Difference Spectrum in the Isocyanate Region: (a) Freshly cast sample and (b) after 4 months aging at room temperature.

Table 2, column 5. The tiny changes in the isocyanates' 2200 cm^{-1} region are documented in Fig. 3c and Table 1. All these changes will be discussed below.

3. THERMAL AGING

The FTIR difference spectrum of the 100°C , 1-hr-aged Uralane 5753 less the starting material is shown in Fig. 4a, b, and c. The difference-spectrum quality is judged to be excellent, for the reasons given above. Here, FCR = 1.80. Much the same results are observed as with physical aging: Below 900 cm^{-1} and above 3050 cm^{-1} , the peaks subtract out exactly. The ratio of the magnitudes of the 911 , 966 , 1220 , 1522 , and 1712 cm^{-1} peak absorbance reductions is $0.28:1.0:0.40:0.66:0.26$, showing significantly different results for the 911 and 1712 cm^{-1} bands, compared with the previous case. In contrast to the physical-aging result for the 911 cm^{-1} difference peak absorbance (-0.78), the thermal-aging result is -2.3 . Furthermore, the physical-aging results near 1375 cm^{-1} (positive) and 1640 cm^{-1} (negative) have subtracted out to zero in the thermal-aging results. Thus, thermal aging seems largely to be accelerated and enhanced physical aging, but with some differences in detail (especially near 1375 and 1640 cm^{-1}). This is borne out by the results in Fig. 4c for the isocyanate region. The meaning of these changes will be discussed below.

4. ELECTRICAL AGING

The FTIR difference spectrum of the 3-month, 24 kVdc (0.125-in. thick) electrically aged Uralane 5753 less the edge material, which had seen essentially zero electric field, is shown in Fig. 5a, b, and c. Here, FCR = 1.30. The purely physical aging effects are therefore subtracted out. The difference spectrum quality is judged to be excellent, for the reasons given above. Much the same results are observed as with physical and thermal aging: Below 900 cm^{-1} and above 3050 cm^{-1} , the peaks subtract out exactly. The ratio of the magnitudes of the 911 , 966 , 1220 , 1522 , and 1712 cm^{-1} peak absorbance reductions is $0.15:1.0:0.16:0.37:0.19$, differing in detail from the previous two cases. In contrast to the previous results for the 966 cm^{-1} peak absorbance (physical = -0.78 , thermal = -2.3), the electrical-aging result is -0.34 . Furthermore, there are some different details in the 990 to 1200 cm^{-1}

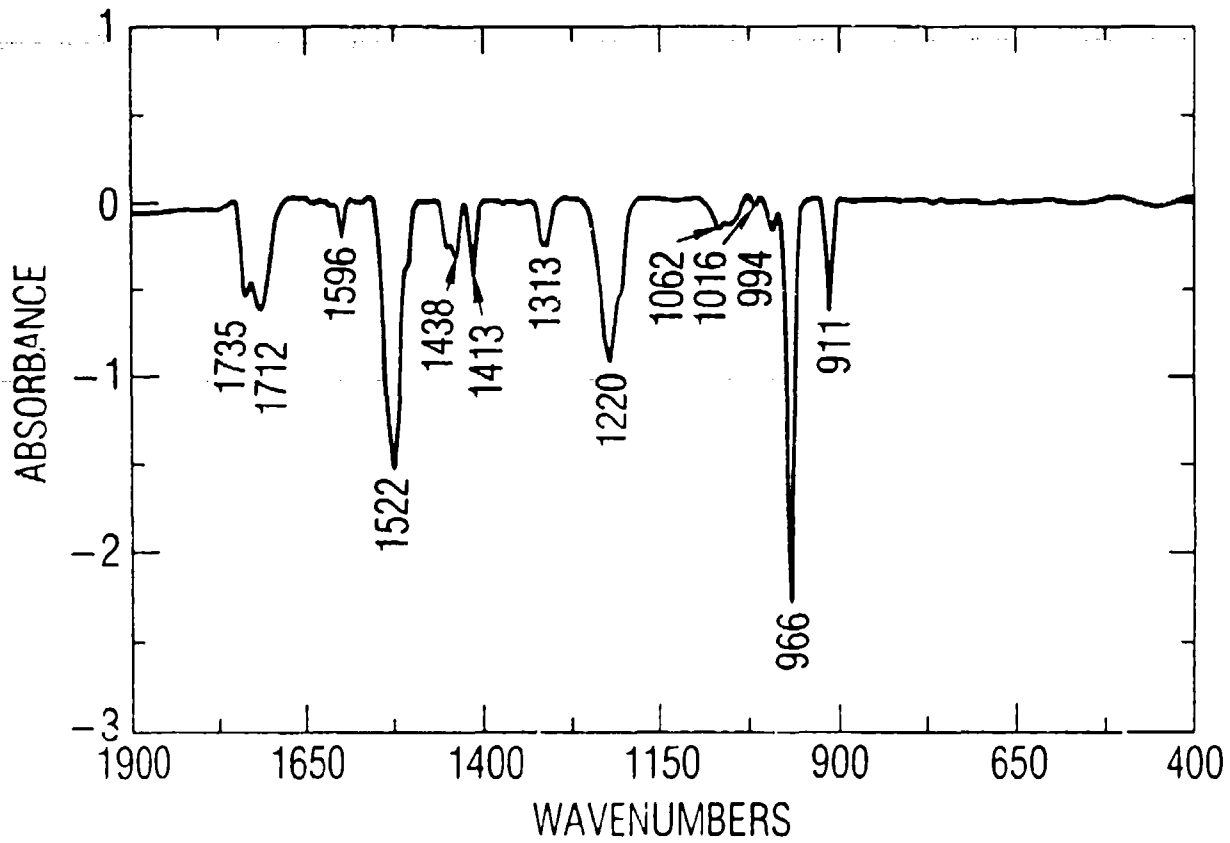


Fig. 4a. Uralane 5753 Thermal-Aging Infrared Difference Spectrum (Lower Frequencies)

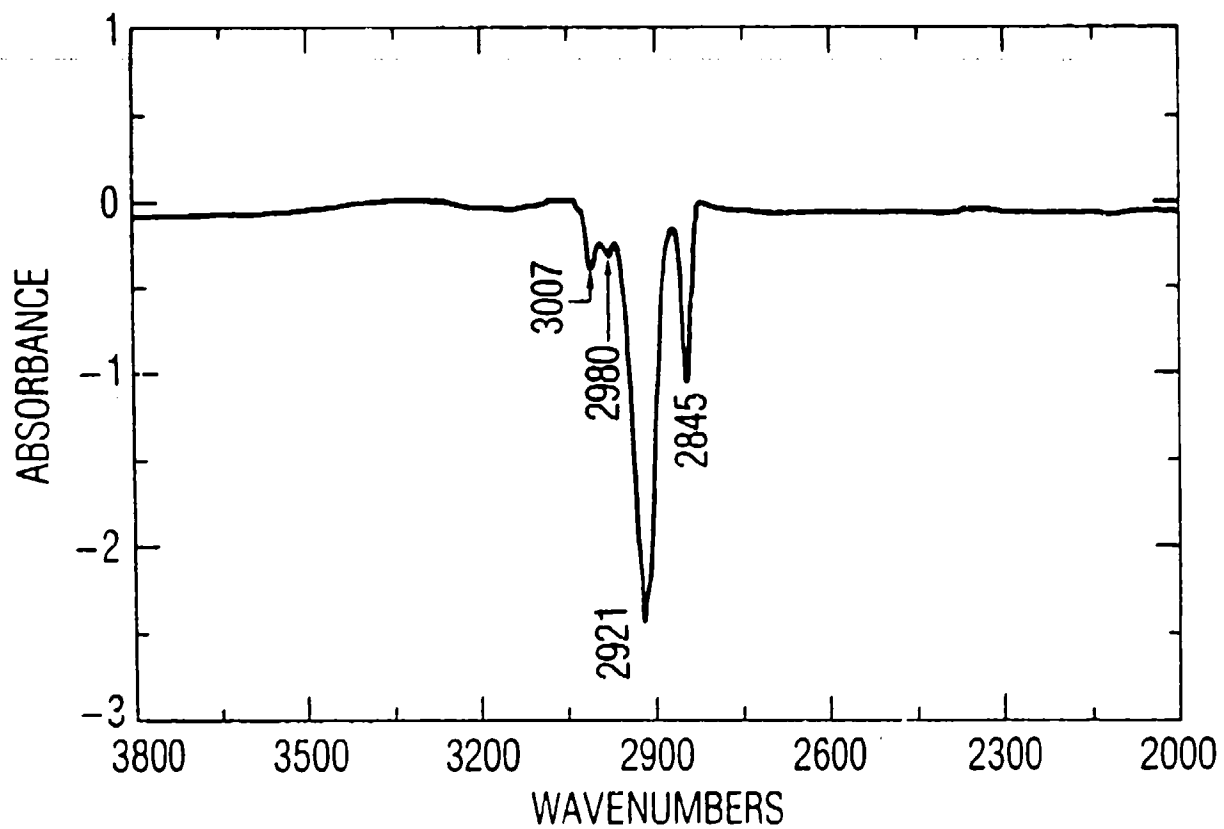


Fig. 4b. Uralane 5753 Thermal-Aging Infrared Difference Spectrum (Higher Frequencies)

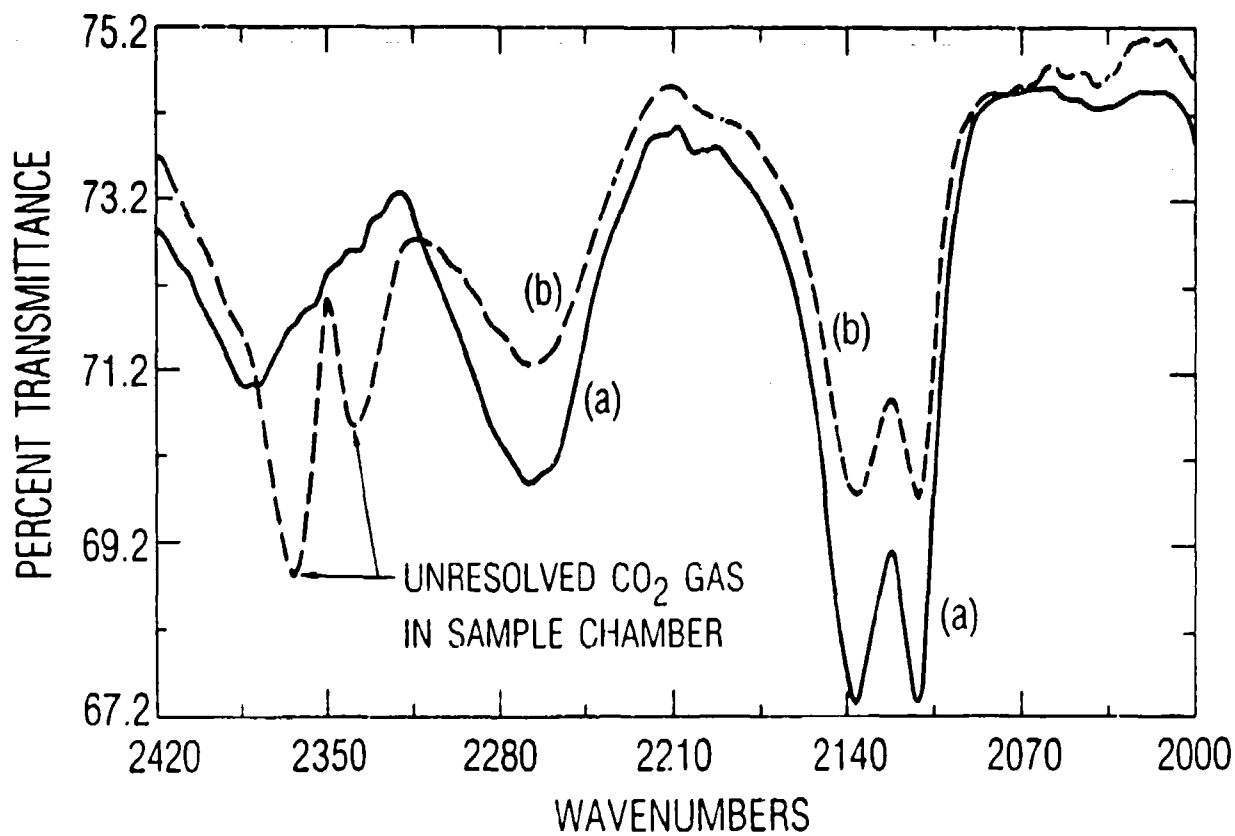


Fig. 4c. Uralane 5753 Thermal-Aging Infrared Difference Spectrum in the Isocyanate Region: (a) Reference sample and (b) thermally-aged sample (including two extraneous, unresolved CO₂ (gas) peaks near 2350 cm⁻¹, which should be ignored).

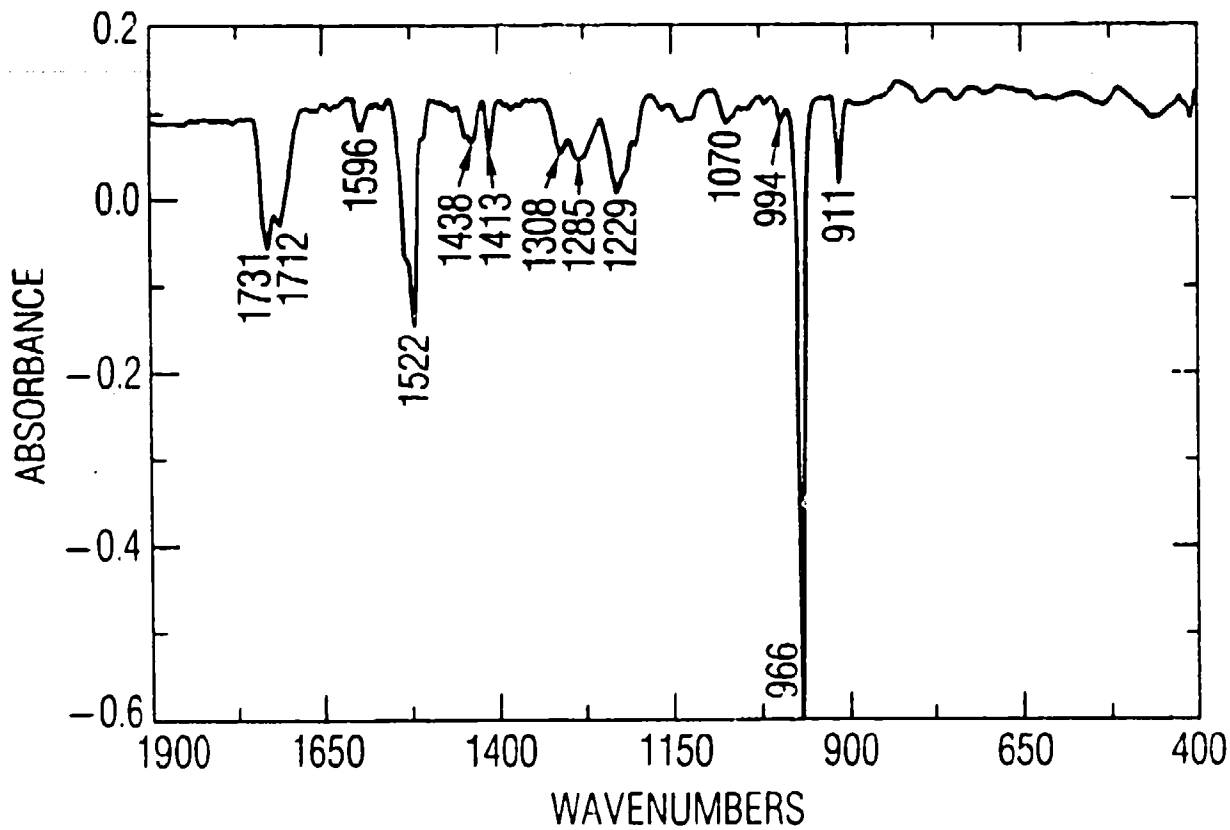


Fig. 5a. Uralane 5753 Electrical-Aging Infrared Difference Spectrum (Lower Frequencies)

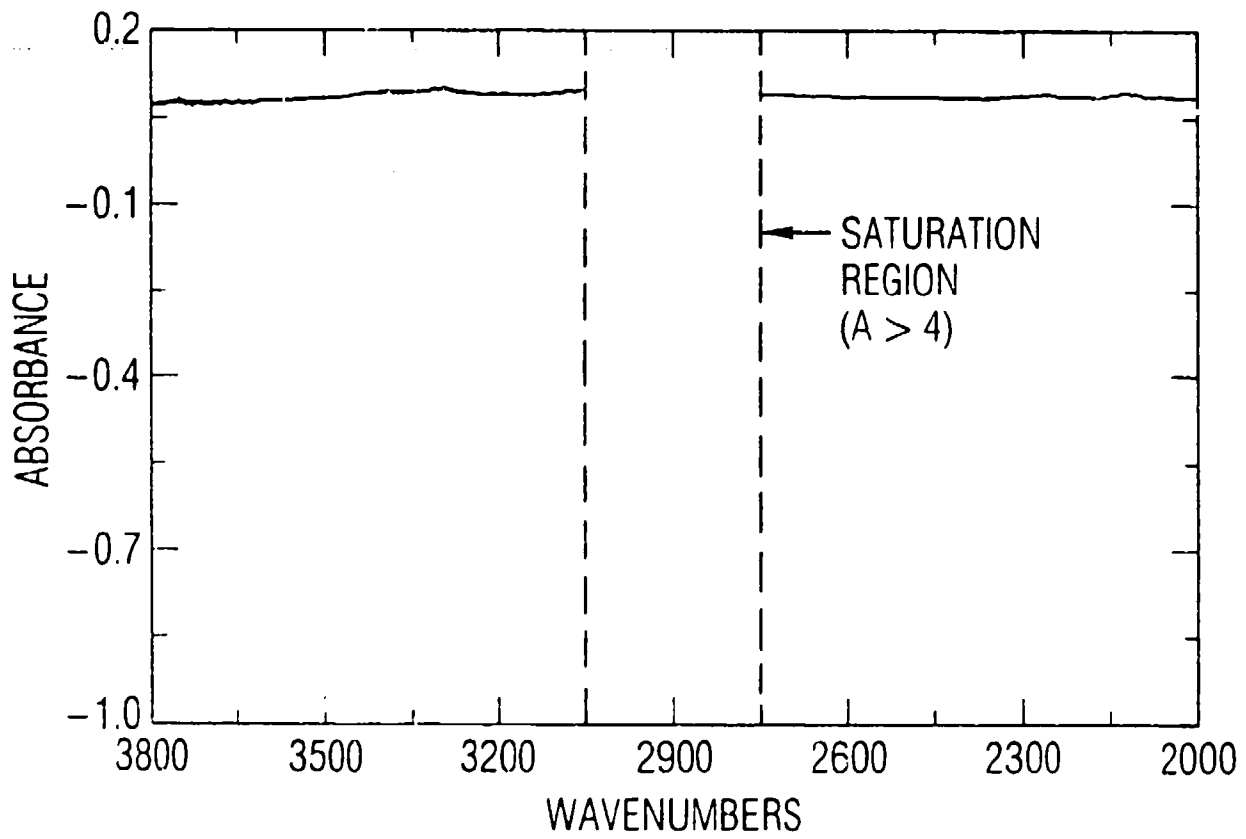


Fig. 5b. Uralane 5753 Electrical-Aging Infrared Difference Spectrum (Higher Frequencies)

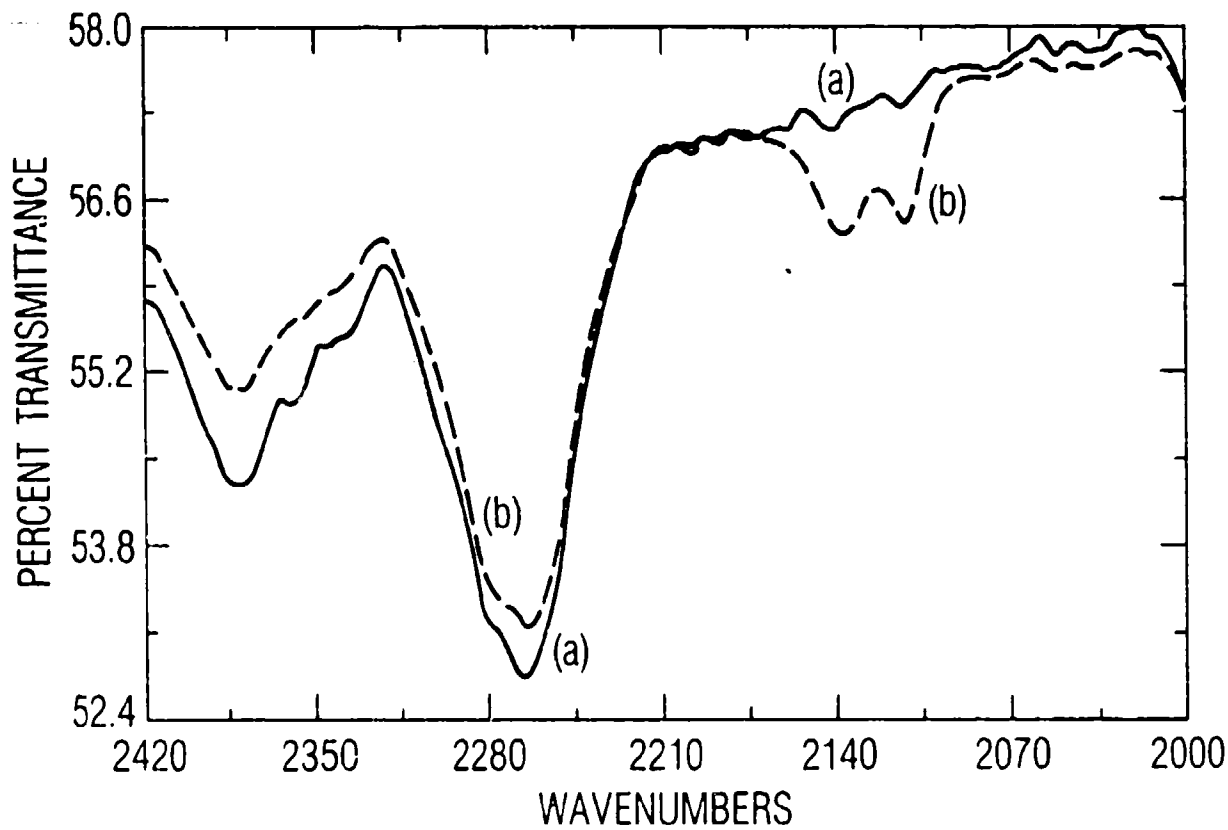


Fig. 5c. Uralane 5753 Electrical-Aging Infrared Difference Spectrum in the Isocyanate Region: (a) Reference sample and (b) electrically-aged sample.

region and the appearance of a negative-going 1280 cm^{-1} peak in this electrical aging result. Thus, while the general nature of electric-field-induced changes are the same as in the case of physical and thermal aging, the relative decrease of the 1220 cm^{-1} absorbance is much less and a new 1280 cm^{-1} absorbance decrease signifies a somewhat different process. This view is supported by the isocyanate-region results in Fig. 5c. The 2137 and 2112 cm^{-1} results are opposite to the physical- and thermal-aging results. Hence, if the state of cure increases during physical and thermal aging, then electrical aging apparently reverses the curing reaction.

IV. DISCUSSION

Since the thermal- and electrical-aging results in Fig. 4a and 5a are substantially similar to the physical-aging results in Fig. 3a, it is a reasonable working hypothesis that these aging methods are achieving substantially the same result by different means. This can be understood as follows.

Because of kinetic limitations during sample preparation, actual polymer samples are typically not in thermodynamic equilibrium. In general, physical aging is expected to be a slow process of overcoming free-energy barriers in order to approach thermodynamic equilibrium. Thermal aging accelerates this approach, because of the increased energy needed to surmount the energy barriers. If there is a mechanism for conduction-band electrons to acquire energy from an applied electric field and to impart that energy to the polymer lattice, then local heating and an accelerated approach to thermodynamic equilibrium also result from electric aging. In the following sections we will inquire as to what chain motions may reasonably be expected in a polymer driven toward thermodynamic equilibrium, as well as to the likelihood that such motions would be accompanied by changes in infrared absorbance.

In the writings of Fröhlich and others it is shown that conduction-band electrons mediate an energy transfer from an applied electric field to the lattice by electron scattering off of inhomogeneities such as free-volume holes or other defects which are expected in a phase-separating system. Our final consideration in this section will be to review the reasons why the proposed molecular motions would likely be accompanied by an increasing rate of electron-mediated energy transfer to the lattice, leading ultimately to ionization, gas formation, and electrical breakdown.

A. CHAIN MOTION, CHAIN CONFORMATION, AND REDUCTION IN IR ACTIVITY

Beer's law states that $A_1 = a_1 b c_1$ where A_1 , a_1 , b , and c_1 are the (i^{th} species) absorbance, infrared activity, sample thickness, and concentration, respectively. In the present experiments the thickness, b , was adjusted mathematically (by using the FCR number) to be constant. Variations in A

could arise from variations in a or c. Discrete chemical reactions may alter concentrations (c), while ordering or changes in the average interchain spacing may alter infrared activities (a). The attribution of difference spectra peaks to changes in a or c will depend on independent knowledge on a case by case basis. Because of our knowledge of the cure system, a discussion of isocyanate absorbance changes (near 2270 cm^{-1}) would involve chemical reactions and concentrations. On the other hand, the 966 cm^{-1} trans-1,4-polybutadiene band in a sample held at room temperature (Fig. 1) would not change unless some "physical," as opposed to a "chemical," change were occurring. There is a precedent for interpreting the changes at 966 cm^{-1} , as well as the other non-isocyanate frequencies, in terms of changes in a, as discussed below.

It is expected that Uralane forms a phase-segregated structure (possibly microdomains that are hundreds of angstroms thick), since the polybutadiene (PBD) is nonpolar while the urethane groups exhibit strong interchain interactions (hydrogen bonding). Figure 1a and b shows the two-phase behavior of Uralane (see also Ref. 32). Initially, a system of hydrogen bridges is formed which exhibits a relatively low level of order. The broad exotherm evident between 160 and 220°C (Fig. 1b) corresponds to a "crystallization," or increase in ordering, upon heating. Therefore we expect time- and temperature-dependent behavior.

The PBD phase in a physically crosslinked system is expected to be mostly amorphous, and it has been shown that the time dependence of the absorbance changes implies that physical rearrangement of chains occurs during thermal aging.³¹ If one considers the propagation of "kinks"³³ along the PBD chain segments to be the cause of (1) reptation in an uncrosslinked system and of (2) the "diffusional" motion of the chain along its own length, then it is also reasonable to expect that kink-propagation could eventually affect the ordering of the amorphous phase of a physically crosslinked system. Kink-propagation could gradually allow the chain to overcome energetic barriers, allowing one chain conformation to be succeeded by another. Depending on time and temperature, the amorphous-phase chain could adopt a more "relaxed" conformation, with corresponding changes in the infrared spectrum.

Such relaxation is not inconsistent with the fact that crosslinking and the interference of vinyl branches prevent actual crystallization. In a crosslinked system much time may be necessary for this relaxation, even if the system temperature is above its hard-domain T_g . Eventually, however, conformational changes are expected in both the polybutadiene and urethane phases, with the corresponding changes in infrared activity.

In summary, then, there are experimental (DSC crystallization evidence between 160 and 220°C) and a priori (kink propagation theory) reasons to expect a changing infrared activity in aging polyurethanes. Experimentally we find generally decreasing infrared absorbance values. In the case of the trans-1,4-PBD band at 966 cm^{-1} , this would be interpreted as the result of a disordering process that reduces the number of trans conformers. The urethane-phase infrared absorbance reduction (for example at 1731, 1712, 1522, and 1220 cm^{-1}) is also consistent with a changing intermolecular environment.

B. MOLECULAR-ENVIRONMENTAL EXPLANATION FOR CHANGING INFRARED ACTIVITY

Another way to describe chain motion from one conformational state to another is in terms of a changing intermolecular environment, which perturbs the chain in such a way as to account for the various observations. Compendia of some of the research on intermolecular-environmental effects in polymers are given in Refs. 34 and 35. For example, Anton³⁶ and Fukawa³⁷ studied infrared absorbances as a function of molecular stress and temperature. Fukawa noted that several peak absorbances in polyvinyl chloride varied with temperature, as did the refractive index or the dielectric constant. Since the dielectric constant is related to the dipole moment, temperature-dependent changes in the dipole moments, especially in polar polymers, are expected to affect infrared absorbances.

Some studies^{38,39} of infrared absorbances in liquids and low-molecular-weight solids related absorbance decreases to thermal expansion. A theoretical treatment^{40,41} of intermolecular-interaction effects upon absorbance predicted that $A_i = A_{i0} + \alpha T$, and α is usually negative. Hannon and Koenig⁴² analyzed PVC absorbance changes with temperature in terms of molecular strain and order.

However, Joss, Bretzlaff, and Wool⁴³ note that significant progress in the quantitative interpretation of infrared intensities has only recently become possible as "the twin-monsters of (dipole derivative) sign ambiguity and of normal coordinates have been reduced in stature from unsolvable to just normally difficult."⁴⁴ Reliable intensity calculations pose state-of-the-art problems in contemporary infrared science. Such calculations for phase-separated systems of reptating (moving via kink propagation) and variably crosslinked chains would be all the more difficult, but it is not surprising that changes in infrared activity occur in such systems.

C. IMPACT OF MOLECULAR MOTION UPON ELECTRONIC PROPERTIES AND ELECTRICAL TREE NUCLEATION

Uralane, as a polymer whose chains are in constant motion according to the above concepts, is susceptible to many long-term energy-transfer processes that can culminate in void formation and electrical tree nucleation after long times.

Temperature-dependent mobility of electrons, impurities, imperfections, phase boundaries, free-volume holes, or polymer chains plays a role in the electric breakdown theories mentioned in Refs. 3 through 21. High-temperature polymer breakdown follows thermal breakdown theory,³ because thermal motion makes the chains appear more like atomic matter to which ordinary dielectric loss and thermal conductivity balance conditions apply. In the Fröhlich microscopic theories,⁵ the relative balance between electron-electron and electron-phonon collisions determines whether or not electrons pick up enough energy from the electric field to ionize polymer atoms or trap sites. Ionization and recombination have been observed near electrical discharge points and may be assumed to occur prolifically before polymer breakdown.

Circumstantial evidence that polymer motion might affect trap-site energetics is the observation¹³ that released molecular motion above polymer transition temperatures results in released charge, as measured by thermally stimulated discharge (TSD). Therefore, the correlation of molecular mobility with charge trapping is real, even if Fröhlich-type theories for moving chains are not available. Electron scattering off newly forming trap sites would

result in ionization or vibrational excitation. "Terminal groups"⁷ would be split off, with the formation of gas, "tree buds," and (after a time lag) electrical trees. Thermionic emission studies⁸ as well as electron-beam irradiation⁹ show that the trapped space charge can exist for long times in polymers, enhancing the electrical stress and energy-transfer to electrons in very localized areas. Gradual disordering and gas formation in these areas can result in electrical tree nucleation.

In addition to the effects related to phase separation, stress cracking by an alternating electrical field¹³ would also be expected to result in time-dependent void formation and electron-scattering properties. Furthermore, any chain-scission process is expected to lead to radical formation and diffusion, a process that may also potentially alter infrared spectra.

V. SUMMARY AND CONCLUSIONS

Electrical breakdown of insulation may occur as a result of macroscopic flaws formed during processing or as a result of long-term molecular degradation. It is often possible to eliminate the macroscopic flaws. On the other hand, it is seen in this report that many experimental results in the literature, as well as the results presented here, are consistent with a picture of polyurethane as a seething molecular cauldron of incessant activity. The polymer chain motion causes the system to pick up more energy from the applied electrical field via electron scattering from the increased number of free-volume hole sites. [Partial ordering in some parts of a crosslinked system produces lower densities (free-volume holes) in other parts.] After a time, which appears indefinite only as long as the system is not adequately characterized, a constant electrical stress may initiate an electrical tree in a system that has been sufficiently weakened by long-term, low-level energy absorption. Several theories were presented which explain changing infrared activity in terms of microscopic polymer motions. Therefore, if the molecular motion, electronic energy transfer, and infrared activity theories are valid, then there is a correlation between the reactivity seen via FTIR and the susceptibility to electrical tree nucleation. In the opinion of the authors, the preponderance of evidence in the literature firmly establishes the scientific validity of these theories, at least in their main features.

The emerging picture from more than 50 years of dielectric research is that electron injection from metal electrode protrusions, as evidenced by electroluminescence¹⁶ and the development of degraded material near those points, is a key feature of the prebreakdown events. Electroluminescence also implies there are electron-hole recombination events, i.e., trap-site energetics are important. Traps also accumulate space charge, enhancing electrical stress and tree formation. Microscopic imperfections, impurities, and free-volume holes may form trap sites, increasing conduction-electron scattering and energy transfer to the lattice. Eventually, a significant number of atoms in polymer chains may become ionized, forming gas, radicals,

and tree nucleation sites. Released molecular motion above T_g and rearrangements of free-volume holes seem to enhance electron transport and breakdown, as evidenced by TSD peaks. Mitsui et al.¹⁵ conducted the first FTIR difference-spectroscopy study of the molecular changes occurring in an electrically stressed epoxy. We studied the formative stage of Uralane 5753 degradation via physical, thermal, and electrical methods. The changes in infrared absorbance noted in Tables 1 and 2 were interpreted as changes in the infrared activity arising from chain motion and what was assumed to be different conformational states. Other theories of intermolecular-environmental effects on infrared activity are possible, as noted above. The changes are enhanced at elevated temperatures, and many of the same changes can occur when the energy is furnished by the electrical field. Hence, infrared spectroscopy can serve as an early-warning system against material changes likely to culminate in catastrophic breakdown.

Phase-separation events occur in polyurethanes to alter microstructure and to provide more sites for electron scattering, thereby increasing susceptibility to electrical tree nucleation. The free-energy driving force, consisting of contributions from hydrogen bonding and entropy effects, causes these changes in the urethane phase. Hindered reptation (i.e., propagation via "kinks") may occur in the soft segment phase. Eventually the typical chain in each phase may possess a different conformation or exist in a different environment. In either case, one expects on a priori grounds that the infrared activity will change, although its exact calculation would pose state-of-the-art problems in infrared science.

Consistent with these views we have documented that observable FTIR changes occur during what Budenstein²¹ has called the formative stage before catastrophic breakdown. For example (see Table 2), the following urethane-phase observations were made: N-H bending and C-N stretching vibrations at 1220 and 1522 cm^{-1} showed strong or medium reductions with physical, thermal, or electrical aging. However, N-H stretching vibrations (3423, 3370, and 3327 cm^{-1}) showed no change, as did the ester-bending vibration at 770 cm^{-1} . (It should be recalled that normal modes are linearly independent excitations of a chain and may behave differently even though they arise from motions within

the same chemical group.) Carbonyl response (1735 and 1712 cm^{-1}) showed a medium reduction. (It should be noted that Wang and Cooper, on p. 682 of Ref. 45, stated that C=O is more affected than the NH group by the formation of three-dimensional hydrogen bonds.)

Corresponding PBD-phase observations were as follows: 1,2-PBD and cis-1,4-PBD bands showed at most medium decreases, while the 966 cm^{-1} trans-1,4-PBD [$(\gamma_w(=CH)_{op})$] band showed a very strong decrease. (In the survey spectrum, the 966 cm^{-1} peak absorbance is about twice that of the 911 cm^{-1} peak. In the difference spectra, the corresponding ratio is between 4 and 8.) Bands due to C-H stretching (2921 and 2845 cm^{-1}) showed strong to very strong decreases, but, being largely independent of the CH_2 group environment, could be due to any type of PBD. Therefore, on balance, it seems that the trans-1,4-PBD exhibits the band with the greatest absorbance decrease and, in our interpretation, the greatest infrared activity decrease due to changes in chain conformation or environment.

Finally, the 2137 and 2112 cm^{-1} isocyanate results are similar in sign for physical and thermal aging but opposite for electrical aging. If the state of cure increases during physical and thermal aging, then electrical aging apparently reverses the curing reaction.

In their shortest form the conclusions are as follows:

1. If the stated theories of molecular motion during aging are true, then aging is expected to lead to reduced infrared activity, as observed.
2. If the stated theories of electronic motion during aging are true, then aging is expected to lead to gradually diminishing resistance to electrical stress.
3. The authors believe that the established theories of molecular and electronic motion are true in their main features.
4. Therefore, the authors believe there is a significant correlation between infrared absorbance decreases and increasing susceptibility to electrical stress. Chain motions occur which may in general affect the infrared activity and result in the formation of free-volume holes or "grain boundaries." Increasing numbers of imperfections increase the energy transfer from electron-scattering events, as well as offer preferred breakdown paths.

5. Therefore, improved (voltage-stabilized) insulation will show fewer infrared absorbance changes during prebreakdown aging. During the chemist's optimization of his formulation, he needs adequate diagnostic tools, one of which is the FTIR technique discussed here and in subsequent reports.

REFERENCES

1. S. L. Zacharius and G. A. Cagle, Proceedings of the International Electronics Packaging Society (1983).
2. (a) R. S. Bretzlaff, S. L. Zacharius, S. L. Sandlin, and C. A. Cagle, Conference on Electrical Insulation and Dielectric Phenomena, Buffalo, NY, IEEE Annual Report (1985) (b) R. S. Bretzlaff, and S. L. Sandlin, International Conference on Conduction and Breakdown in Solid Dielectrics, Erlangen, W. Germany (1986).
3. B. L. Goodlet, F. S. Edwards, and F. R. Perry, J. Instn. Electr. Engrs. 69, 695 (1931).
4. J. J. O'Dwyer, The Theory of Electrical Conduction and Breakdown in Solid Dielectrics (Clarendon Press, Oxford, 1973).
5. H. Fröhlich, Proc. Roy. Soc. A160, 230 (1937); A188, 521, 532 (1947).
6. K. H. Stark and C. G. Garton, Nature 176, 1225 (1955).
7. B. Yoda and M. Sakaba, Hitachi Review 18, 406 (1969).
8. D. M. Taylor and T. J. Lewis, J. Phys. D4, 1346 (1971).
9. C. M. Cooke, E. Williams and K. A. Wright, IEEE Int. Symp. on Electr. Insul., Conf. Record (1982), p. 95.
10. R. M. Eichorn, IEEE Trans. EI-2, 2 (1976).
11. A. C. Ashcraft, R. M. Eichorn, and R. G. Shaw, IEEE Int. Symp. on Electr. Insul., Conf. Record (1976), p. 213.
12. G. Bacquet, J. Dib, C. Y. Wu, M. R. Wethermer, A. Yelon, J. R. Deusley, and S. A. Boggs, IEEE Trans. EI-13, 157 (1978).
13. M. Ieda, IEEE Trans. EI-15, 206 (1980).
14. T. Mizutani, Y. Suzuoki, and M. Ieda, J. App. Phys. 48, 2408 (1977).
15. H. Mitsui, T. Yoshimitsu, Y. Mizutani, and K. Umemoto, IEEE Trans. EI-16, 533 (1981).
16. N. Shimizu, J. Katsukawa, M. Miyauchi, M. Kosaki, and D. Horii, IEEE Trans. EI-14, 256 (1979).
17. O. Dorlante, S. Sapicha, M. R. Wertheimer, and A. Yelon, IEEE Trans. EI-17, 199 (1982).

18. J. M. Schultz and C. Lyhmn, Polymer Composites 7, 215 (1984).
19. J. J. O'Dwyer, IEEE Trans. EI-17, 484 (1982).
20. J. J. O'Dwyer, IEEE Trans. EI-15, 264 (1980).
21. P. P. Budenstein, IEEE Trans. EI-15, 225 (1980).
22. J. Saunders and K. Frisch, Polyurethanes: Chemistry and Technology, (Robert Krieger, Huntington, New York, 1978).
23. E. Doyle, The Development and Use of Polyurethane Products (McGraw-Hill, New York, 1971).
24. P. Bruins, Polyurethane Technology (Interscience, New York, 1969).
25. J. L. Willet and R. P. Wool, Bulletin of the Amer. Phys. Soc. EV-12 (March 1985).
26. R. S. Bretzlaff, S. L. Zacharius, S. L. Sandlen, and G. A. Cagle, FTIR Study of Aging in Commercial Polyurethane, TR-0086(6925-08)-3, Aerospace Corporation (28 April 1986).
27. R. S. Bretzlaff and T. B. Bahder, preprint accepted by Revue de Physique Appliquée, to appear in December, 1986.
28. C. M. Brunette, S. L. Hsu, and W. J. MacKnight, Poly. Engr. and Sci. 21, 163 (1981).
29. Sadtler Infrared Spectra Atlas of Monomers and Polymers (1980).
30. S. W. Cornell and J. L. Koenig, Macromolecules 2, 540 (1969).
31. R. S. Bretzlaff, T. B. Bahder, and S. L. Sandlin, preprint submitted to IEEE Trans. on Electr. Insulation (April 1986).
32. R. Bonart, J. Macromolec. Sci., Phys. B2, 115 (1968).
33. P. de Gennes, J. Chem. Phys. 55, 572 (1971).
34. B. L. Joss, M. S. Thesis, University of Illinois, Urbana (1984).
35. R. S. Bretzlaff, Ph.D. Thesis, University of Illinois, Urbana (1984).
36. A. Anton, J. Appl. Polym. Sci. 12, 2117 (1968).
37. K. Fukawa, J. Chem. Soc. Japan 66, 1605 (1963).
38. T. L. Brown, J. Chem. Phys. 24, 1281 (1956).
39. M. P. Lisita and Y. P. Tsyaschenko, Opt. Spektrosk. 9, 229 (1960).

40. L. N. Ovander, Opt. Spektrosk. 11, 68 (1961).
41. L. N. Ovander, Opt. Spektrosk. 12, 401 (1962).
42. M. J. Hannon and J. L. Koenig, J. Polym. Sci. A2-7, 1085 (1969).
43. B. L. Joss, R. S. Bretzlaff, and R. P. Wool, J. Polym. Engr. and Sci. 24, 1130 (1984).
44. B. Crawford, Jr., in Vibrational Intensities in Infrared and Raman Spectroscopy, Ch. 1, W. B. Person and G. Zerbi, eds. (Elsevier, Amsterdam, 1982).
45. C. B. Wang and S. L. Cooper, Macromolecules 16, 775 (1983).

LABORATORY OPERATIONS

The Aerospace Corporation functions as an "architect-engineer" for national security projects, specializing in advanced military space systems. Providing research support, the corporation's Laboratory Operations conducts experimental and theoretical investigations that focus on the application of scientific and technical advances to such systems. Vital to the success of these investigations is the technical staff's wide-ranging expertise and its ability to stay current with new developments. This expertise is enhanced by a research program aimed at dealing with the many problems associated with rapidly evolving space systems. Contributing their capabilities to the research effort are these individual laboratories:

Aerophysics Laboratory: Launch vehicle and reentry fluid mechanics, heat transfer and flight dynamics; chemical and electric propulsion, propellant chemistry, chemical dynamics, environmental chemistry, trace detection; spacecraft structural mechanics, contamination, thermal and structural control; high temperature thermomechanics, gas kinetics and radiation; cw and pulsed chemical and excimer laser development including chemical kinetics, spectroscopy, optical resonators, beam control, atmospheric propagation, laser effects and countermeasures.

Chemistry and Physics Laboratory: Atmospheric chemical reactions, atmospheric optics, light scattering, state-specific chemical reactions and radiative signatures of missile plumes, sensor out-of-field-of-view rejection, applied laser spectroscopy, laser chemistry, laser optoelectronics, solar cell physics, battery electrochemistry, space vacuum and radiation effects on materials, lubrication and surface phenomena, thermionic emission, photo-sensitive materials and detectors, atomic frequency standards, and environmental chemistry.

Computer Science Laboratory: Program verification, program translation, performance-sensitive system design, distributed architectures for spaceborne computers, fault-tolerant computer systems, artificial intelligence, micro-electronics applications, communication protocols, and computer security.

Electronics Research Laboratory: Microelectronics, solid-state device physics, compound semiconductors, radiation hardening; electro-optics, quantum electronics, solid-state lasers, optical propagation and communications; microwave semiconductor devices, microwave/millimeter wave measurements, diagnostics and radiometry, microwave/millimeter wave thermionic devices; atomic time and frequency standards; antennas, rf systems, electromagnetic propagation phenomena, space communication systems.

Materials Sciences Laboratory: Development of new materials: metals, alloys, ceramics, polymers and their composites, and new forms of carbon; non-destructive evaluation, component failure analysis and reliability; fracture mechanics and stress corrosion; analysis and evaluation of materials at cryogenic and elevated temperatures as well as in space and enemy-induced environments.

Space Sciences Laboratory: Magnetospheric, auroral and cosmic ray physics, wave-particle interactions, magnetospheric plasma waves; atmospheric and ionospheric physics, density and composition of the upper atmosphere, remote sensing using atmospheric radiation; solar physics, infrared astronomy, infrared signature analysis; effects of solar activity, magnetic storms and nuclear explosions on the earth's atmosphere, ionosphere and magnetosphere; effects of electromagnetic and particulate radiations on space systems; space instrumentation.